Axial and Radial Solids Distribution in a Long and High-Flux CFB Riser

J. H. Pärssinen and J.-X. Zhu
Dept. of Chemical and Biochemical Engineering, University of Western Ontario, London, Ont., Canada, N6A 5B9

Radial solids concentration profiles were determined with a fiber-optic probe on eight axial levels in a 76-mm-ID, 10-m riser, at solids flux (solids circulation rate) up to 550 kg/m^2·s and superficial gas velocity up to 10 m/s. Radial concentration profiles at high solids fluxes of over 300 kg/m^2·s are less uniform than lower fluxes of less than 200 kg/m^2·s. Under all operating conditions, the flow development in the riser center is nearly instant, with the solids concentration remaining low at the riser center throughout the riser. In the wall region, increasing solids flux significantly slows down the flow development, with the solids concentration near the wall decreasing all the way toward the riser top at high fluxes. In the high-flux circulating fluidized bed (HFCFB), a middle section with intermediate solids holdups of about 7 to 20% was between the bottom dense section and top dilute section, with its length increasing as the solids circulation rate increases and as the gas velocity decreases. Flow conditions in this section resemble those of the dense suspension upflow under high-density operating conditions by Grace et al. (1999). When its length extends to the riser top, a high-density circulating fluidized bed for which an HFCFB is a necessary but not a sufficient condition, forms.

Introduction

Fluidized catalytic cracking (FCC) units have been considered the most successful application of circulating fluidized beds (CFB) in the past decades. The total worldwide capacity of FCC units has increased to over 16 million bbl/d (2#540ML/d), whereas the uplift (difference between the values of products and feeds) could be as high as U.S. $10/bbl (64/L) across the FCC unit (Avidan, 1997). Nearly all FCC units in operation utilize a riser reactor, where the solids circulation rate could range from 400 kg/m^2·s to 1,200 kg/m^2·s and the superficial gas velocity from 6 m/s to 28 m/s, increasing with the height (Zhu and Bi, 1995). In addition, there are also some rising applications of high-flux CFB, such as duPont's production of maleic anhydride (Contractor et al., 1994). Therefore, more research is required at high solids fluxes to improve and optimize the existing industrial CFBs and enhance the design of novel applications (Bi and Zhu, 1993).

Several hundreds of studies on CFB hydrodynamics have been carried out at low solids fluxes of less than 200 kg/m^2·s, whereas only a few limited but useful studies have explored the pilot or industrial risers achieving high solids fluxes of over 500 kg/m^2·s as summarized in Table 1 (van Zoonen, 1962; van Swaaij et al., 1970; Azzi et al., 1991; Martin et al., 1992; Contractor et al., 1994; Knowlton, 1995; van Landeghem et al., 1996; Pugsley et al., 1996; Karri and Knowlton, 1999). Some of the most comprehensive research work of a high-density (and high-flux) riser has been carried out by Issangya et al. (1997a,b; 1998, 1999, 2000, 2001), Issangya (1998), and Liu et al. (1999) at the University of British Columbia (UBC). In their work, it was found that under high fluxes and suspension densities the axial solids concentration profile was fairly flat and the solids net flow direction was primarily upwards at the riser wall. That was clearly different from the previous observations of fast fluidization (FF) regime. Thus, the operations with a higher solids flux than 200 kg/m^2·s combined with a cross-sectional solids concentration of over 10% throughout the riser were defined as a Dense Suspension Upflow (DSU) flow regime (Grace et al., 1999). In comparison to those studies carried out in the DSU regime, the current work will discuss high-flux operations where the axial solids holdup profile is not flat and the cross-sectional solids

Correspondence concerning this article should be addressed to J.-X. Zhu.
J. H. Pärssinen is visiting from Helsinki University of Technology.

Table 1. Studies on Laboratory- and Industrial-Scale CFB Risers with Solids Circulating Rate Exceeding 500 kg/m^2·s

Authors	Height (m)	Dia. (m)	G_s (Max) (kg/m^2·s)	U_g (Max.) (m/s)	Particles	Meas. Techniques
Arena et al. (1988)	6.4	0.041	600	7.0	Glass beads	Quick-closing valves, pressure transducers
Azzi et al. (1991)*	30.0	0.70	1080	21.0	FCC	Gammetry
Contractor et al. (1994)	27.0	0.15	590	7.8	FCC	Not reported
Karri and Knowlton (1995)	13.0	0.30	586	~ 13.5	FCC	Suction probe, pressure transducers
Pugsley et al. (1996)	5.0	0.05	700	8.5	Sand	Pressure transducers
This study	10.0	0.076	550	10.0	FCC	Optic-fiber probe, pressure transducers
Viitanen (1993)*	39.0	1.0	485	13.0	FCC	Radioactive tracing

*Industrial FCC unit.

concentration is clearly less than 10% in the upper portion of the riser. Consequently, the operation has similarities to both DSU and FF flow regimes. Since the cross-sectional solids concentration is also low ($< 10\%$) in the upper portion of most industrial FCC risers, another aim of this work is to provide a detailed image of the radial solids concentration profiles and their development toward the top of a high-flux riser.

Experimental Apparatus

The CFB system is shown in Figure 1. The system consists of two 10-m risers, 76-mm ID, and 203-mm ID, which utilize the same downcomer (storage vessel) with an internal diameter of 0.32 m. The solids were FCC catalyst with a mean diameter of 67 μm and a particle density of 1,500 kg/m^3. The total solids inventory was approximately 350 kg, equivalent to a solids level of approximately 5 m in the downcomer when all solids are stored in the downcomer. For the current work the measurements were done only in the 76-mm-ID riser. The humidity level of the air was controlled between 70 and 80% to eliminate the electrostatics in the system.

After passing a butterfly valve, the solids entered the riser bottom at a height of 0.17–0.25 m, and were accelerated by air in ambient conditions. The gas–solids suspension traveled up in the column and passed the smooth exit into the primary cyclone. The gas was separated further from the solids in the secondary and tertiary cyclones before the gas was sent to a bag filter for final cleaning. From the bottom of the large-capacity bag filter the fine particles collected could be returned back into the downcomer. A solids flow-rate measuring device located inside the top part of the downcomer sections the column into two halves, with a central vertical plate and with two half butterfly valves fixed at the top and the bottom of the two-half section. By appropriately flipping the two valves from one side to the other, solids circulated through the system can be accumulated in one side of the measuring section for a given time period to provide the solids circulating rate.

The local solids concentration was measured with a reflective-type fiber-optic concentration probe. The 3.8-mm-diameter probe tip consisted of approximately 8000 emitting and receiving quartz fibers, each having a diameter of 15 μm. The active area, where the fibers were located, was approximately 2 mm×2 mm. More details of this probe and its calibration can be found in Zhang et al. (1998). The solids concentration in the current study was measured at 11 radial positions (r/R = 0.00, 0.16, 0.38, 0.50, 0.59, 0.67, 0.74, 0.81, 0.87, 0.92, and 0.98) on eight axial levels (z = 1.53, 2.73, 3.96, 5.13, 5.90, 6.34, 8.74 and 9.42 m) under the six operating conditions given in Table 2. At each location, the measurements were carried out at least twice, each over a 30-s period with a sampling frequency of 1,000 Hz, yielding 30,000 data

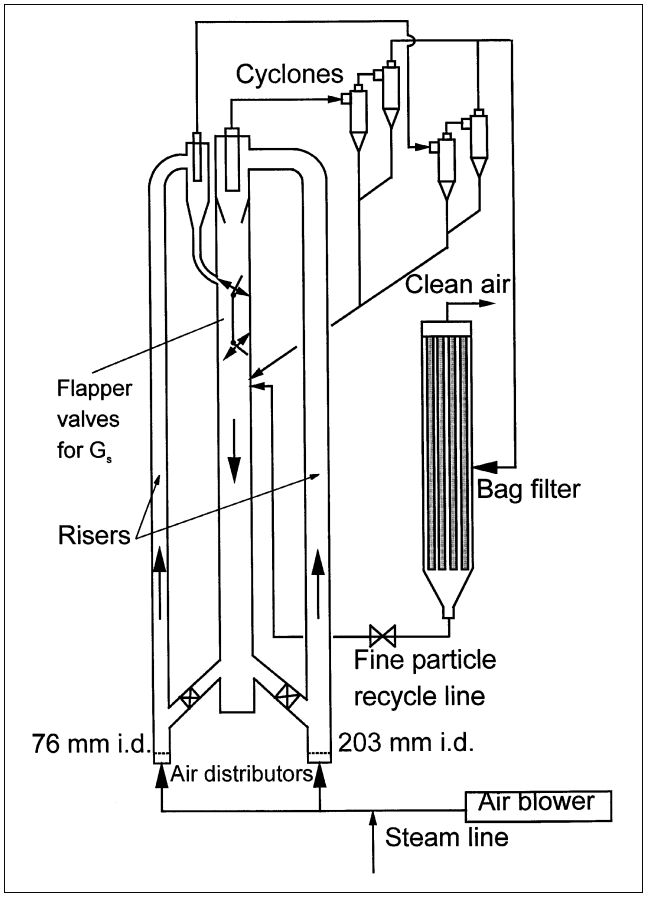

Figure 1. High-flux circulating fluidized-bed system.

Table 2. Operating conditions

Superficial Gas Vel. (m/s)	Solids Circ. rate (kg/m^2·s)
5.5	300
8.0	100
8.0	300
8.0	400
8.0	550
10.0	300

points. The particle velocity was also measured in the same positions and at the same operating conditions with a fiber-optic particle velocity probe consisting of two light-emitting and three light-receiving fibers. For details about this probe and its calibration, please refer to Zhu et al. (2001). By combining the results from these two separate measurements at each axial elevation, the local solids net flux could be obtained.

Results and Discussion

Radial profiles of solids holdup in the high-flux riser

Radial profiles of solids concentration (solids holdup) on eight axial elevations under the five high-flux operating conditions are shown in Figure 2. In general, the solids concentration is higher in the lower section than in the upper section of the riser at all radial positions, and is lower in the center than in the wall region of the riser at all axial locations. In the riser bottom, the solids concentration increases significantly toward the wall, often reaching values as high as 40–50%. Toward the riser top, the solids concentration in the wall region decreases, typically reaching a value of less than 15% in the upper developed section. Increasing solids circulation rate (overall solids flux), G_s, and/or decreasing the superficial gas velocity, U_g, increases the height of the bottom flow development section. Decreasing the superficial gas velocity also increases the solids holdup in the wall region throughout the riser length, but a similar effect is not clearly seen with increasing solids circulation rate in the typical radial profiles in the bottom section and the fully developed section.

In the riser bottom section, the radial variation appears to have three regions under most operating conditions: a central region up to $r/R \approx 0.5$–0.6, where the holdup is low and relatively constant with a gradual increase going outwards, an intermediate region between $r/R \approx 0.5$–0.6 and $r/R \approx 0.8$–0.9, where the solids holdup increases significantly, and a wall region where the solids holdup is high and its increase with the radial position becomes more gradual again. This is different from most of the previous studies on low-flux risers (Bader et al., 1988; Tanner et al., 1994; Schlichthaerle and Werther, 1999), where the radial profiles in the bottom section show a flat central region and a wall region where the solids holdup increases sharply toward the wall. However, our result is similar to the results of Wei et al. (1998), where the solids flux is not higher than 200 kg/m^2·s but the average solids holdup is very high (up to 0.25). At locations immediately above the

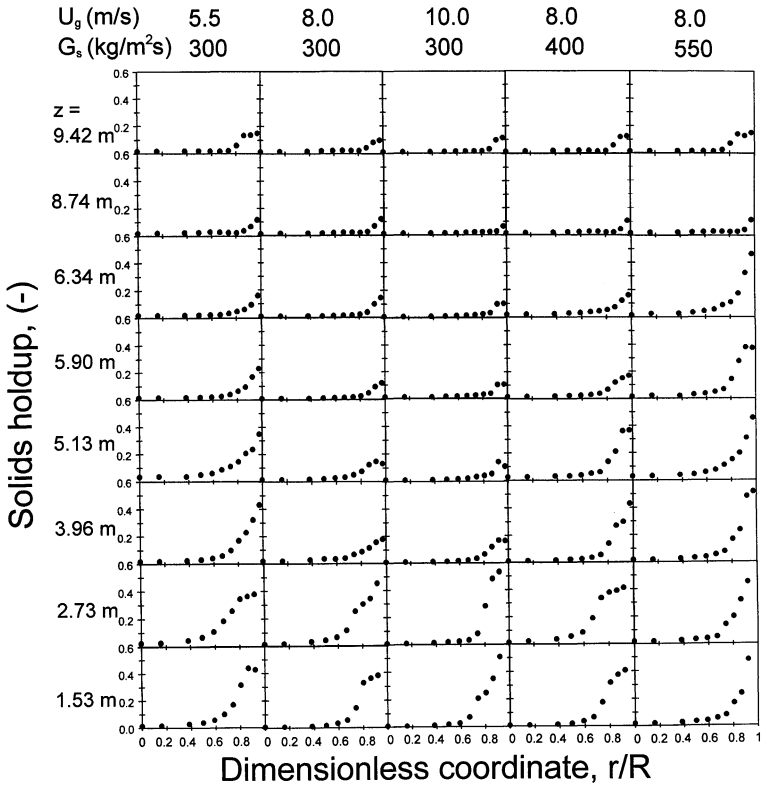

Figure 2. Radial solids holdup profiles under high solids fluxes on eight axial levels.

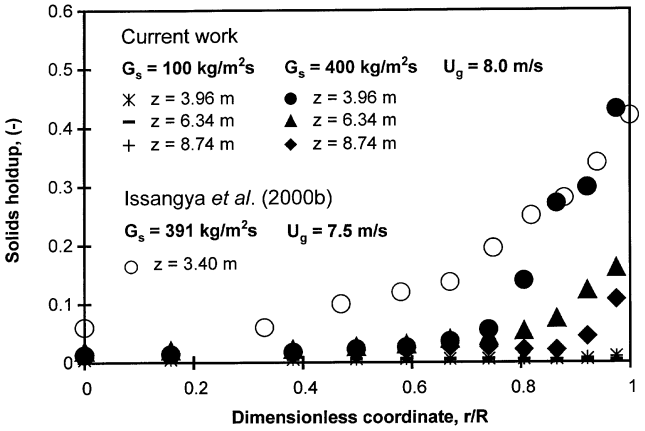

Figure 3. Radial solids holdup profiles at high ($G_s = 400$ kg/m$^2\cdot$s) and low ($G_s = 100$ kg/m$^2\cdot$s) solids fluxes.

solids feeding level, Yang et al. (1997) also found this three-region radial structure with various inlet structures under higher solids holdups reaching 0.30 or more, although the solids flux was less than 130 kg/m$^2\cdot$s. Similar results were also reported by Issangya et al. (2000) in a high-density riser where both solids flux and average solids holdup are high. From the preceding comparison, it seems that it is the higher solids holdup (> 0.20) in the bottom section that determines the three-region radial structure of the solids holdups in the bottom section of the riser.

In the upper section of the high-flux riser, the solids concentration in the wall region is lower than that in the bottom section, typically only reaching a value of less than 15% for high-flux conditions below the riser exit (Figure 3). Compared to those obtained at lower G_s in the same riser, the radial profiles at high solids flux are remarkably less uniform. Compared to the results obtained in the high-density riser at $z = 3.40$ m and G_s 391 kg/m$^2\cdot$s (Issangya et al., 2000), the current results show a similar trend at $z = 3.96$ m and $G_s =$ 400 kg/m$^2\cdot$s. However, the current results show a somewhat wider central region and then a sharp rise in the solids holdup toward the wall. That is likely due to the higher average solids holdup in their riser achieved with much higher solids inventory. On the other hand, our results are closer to the profiles that have been measured in industrial high-flux risers (Martin et al., 1992; Sapre et al., 1992; Derouin et al., 1997), where the average solids holdups are not as high as those of Issangya et al. (2000).

Flow development in the high-flux riser

Figure 2 also provides enough information to examine the solids flow development in terms of its radial solids distributions. If the radial profiles at the 9.42-m level are excluded due to the minor exit effect (even though the exit is a smooth one), the solids flow can be considered fully developed if the radial solids distribution no longer changes with the axial location. With this criterion, it is clearly seen that increasing superficial gas velocity shortens the length of flow development, with a more significant reduction of flow development

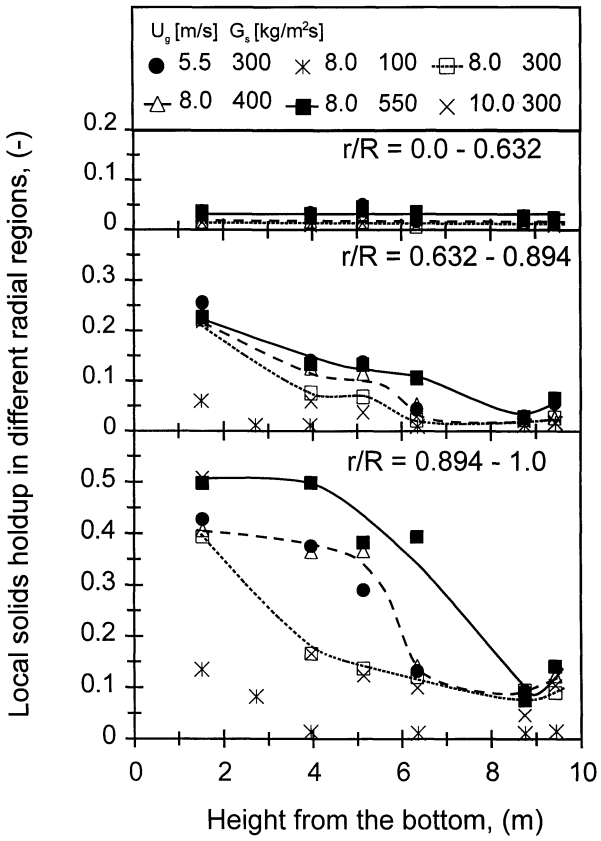

Figure 4. Solids holdup in different radial regions, showing flow development along the riser under various solids fluxes.

when U_g changes from 5.5 m/s to 8.0 m/s than from 8.0 m/s to 10.0 m/s. On the other hand, when the solids circulation rate is increased from $G_s = 300$ kg/m$^2\cdot$s to 400 kg/m$^2\cdot$s and then to $G_s = 550$ kg/m$^2\cdot$s at a constant $U_g = 8$ m/s, the flow development becomes remarkably slower.

Figure 2 also shows that the solids concentration in the riser center remains nearly constant throughout the riser under each operating condition. Figure 2 further shows that even with the change of operating conditions, the solids concentration in the riser center does not seem to change significantly within the tested range of operating conditions. As a result, the flow development is mostly represented by the reduction of the solids concentration toward the riser top at r/R from about 0.50 to 1.00. Similar phenomena can also be seen from the results of Issangya et al. (2000), who showed radial solids concentration profiles on four elevations under $U_g = 6.6$ m/s with $G_s = 234$ kg/m$^2\cdot$s.

To further analyze the solids flow development, the axial profiles of solids holdups in the three radial regions, $r/R =$ 0.0–0.632, 0.632–0.894, and 0.894–1.0, are given in Figure 4. The figure clearly reveals the difference in the flow development in the three radial regions. In the central region ($r/R =$ 0.0–0.632) the solids holdup is very low and nearly constant all the way from the riser bottom to the riser top. In the middle region ($r/R = 0.632$–0.894), on the other hand, the solids holdup first decreases sharply with increasing height

till approximately 4 m, and then more gradually toward the riser top. Except for the situation with the highest solids circulation rate of 550 kg/m^2·s, the solids concentration in this region does not change beyond approximately $z = 6$ m. Most significant variations of the solids holdup happen in the wall region ($r/R = 0.894–1.0$), where the solids concentration drops dramatically from about 40% at the riser bottom to about 10% to 15% at the riser top. Compared to the middle region, the flow in the wall region takes a greater distance to develop and more changes occur in the lower developing section at the riser bottom. Again, the flow is most developed at the 6-m level, except for $G_s = 550$ kg/m^2·s. Figure 4 also more clearly shows that increasing G_s significantly slows down the flow development process, while increasing U_g accelerates it. It can also be noted that increasing U_g from 8 m/s to 10 m/s produces a much lesser effect than increasing the same from 5 m/s to 8 m/s, possibly because a lesser change in overall solids holdup is experienced when increasing U_g from 8 m/s to 10 m/s.

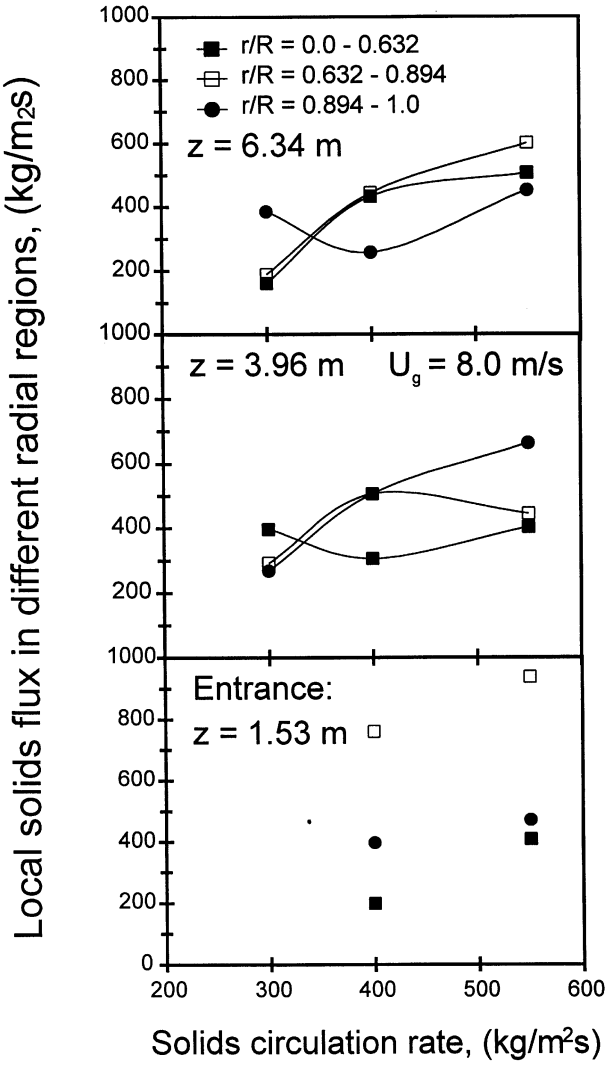

Figure 5. Solids flux in different radial regions at three axial levels.

Indicates that the net solids flux is clearly upwards at all radial regions at high solids fluxes.

Figure 4 also indicates that the solids concentration in the riser center is typically less than 3% all the way from the riser bottom to the riser top. On the other hand, the solids concentration at the wall is very high and is typically between 10% and 20% in the developed section. These values are consistent with the data reported previously by Knowlton (1995) that the solids concentration was less than 3% in the riser center and approximately 18% at the wall under $U_g = 11$ m/s and $G_s = 782$ kg/m^2·s at about 4 m from the riser distributor. Derouin et al. (1997) also obtained similar concentration profiles under $U_g = 6.7$ m/s and $G_s = 303$ kg/m^2·s at a height of about 6 m. On the other hand, Issangya et al. (2000) found a solids concentration of more than 6% in the riser center under $U_g = 6.6$ m/s and $G_s = 234$ kg/m^2·s throughout their entire 6.3-m high riser. Their values may result from the very high solids inventory and high back pressure from the downcomer.

Local solids flux can be calculated from the local solids holdup and particle velocity, which is given in detail elsewhere (Pärssinen and Zhu, 2001). Figure 5 shows the change of net solids fluxes in the three radial regions with the solids circulation rate, on three axial elevations ($z = 1.53$, $z = 3.96$ m, and $z = 6.34$ m) with a constant U_g of 8 m/s. It can be observed that in a high-flux riser ($G_s \geq 300$ kg/m^2·s) the direction of the net solids flux is always upwards in the wall region ($r/R = 0.894–1.0$), as well as at the center. Similar situations were also observed under other high-flux operating conditions in this study. These results are consistent with the results of Karri and Knowlton (1999) and Issangya et al. (1997a) obtained in high-flux and high-density risers. At the lower levels of 1.53 and 3.96 m, the net solids flux is even higher in the wall region compared to the riser center. It is also interesting to note that at a height of 6.34 m the radial distribution of the net solids flux becomes more uniform for the high G_s of 550 kg/m^2·s, compared to lower G_s and compared to that at a height of 3.96 m. This is most likely due to the flow development: the solids concentration is still very high near the wall at 6.34 m (see Figure 4), which compensates for the low particle velocity.

One-dimensional slip velocity

The one-dimensional slip velocity, that is, the average gas velocity $U_g/(1 - \epsilon_s)$ minus the average particle velocity $G_s/(\epsilon_s \rho_p)$, is an indicator of the degree of particle aggregation (Bi et al., 1993) as well as a design parameter (Patience et al., 1992; Pugsley et al., 1994; Berruti et al., 1995). Issangya et al. (1999) have examined the one-dimensional slip velocity in a high-density riser and found it to decrease with U_g and increases with G_s at lower G_s, and then it reaches a constant at higher G_s. Some results from our current study in the high-flux riser are different than theirs.

Plotted in Figure 6 are the variations of the one-dimensional slip velocity along the riser under the five high-flux operating conditions. The first observation is that the one-dimensional slip velocity is very high at the riser bottom and decreases gradually to a lowest value of 2–4 m/s near the smooth exit, reflecting the flow development along the riser. The corresponding slip factor, that is, the average gas velocity $U_g/(1 - \epsilon_s)$ divided by the average particle velocity

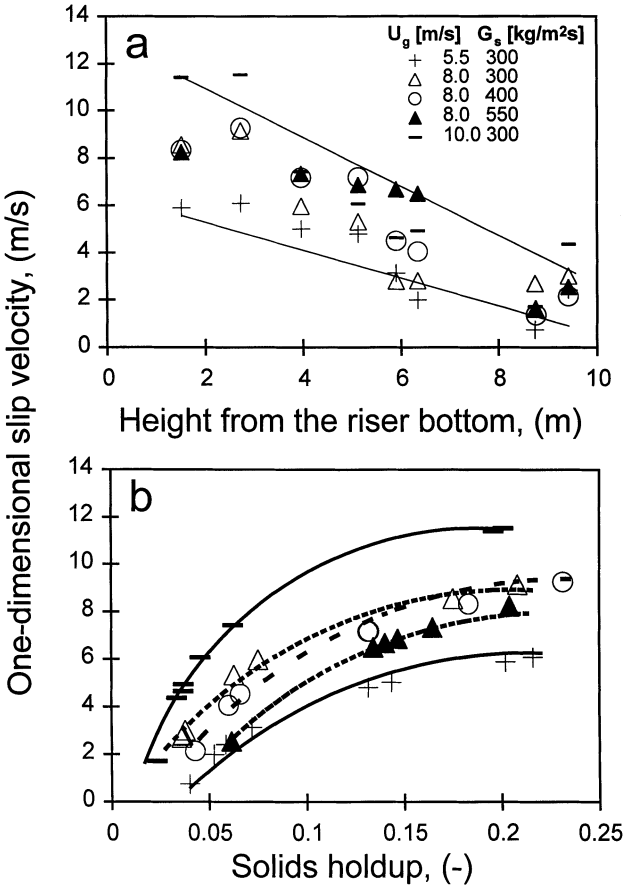

Figure 6. Variation of 1-D slip velocity with (a) axial location and (b) cross-sectional mean solids holdup.

$G_s/(\epsilon_s \rho_p)$, are typically between 6 and 10 in the bottom section and between 1.3 and 4 in the upper dilute section. Compared to the literature data, Matsen (1976) reported values of ~ 2 for the slip factor in the dilute section of an industrial FCC riser, Ouyang and Potter (1993) presented a value of 2.6 based on the pilot scale experiments at fast fluidization regime, and Patience et al. (1992) suggested a value of 2. Those results agree with our results obtained near the riser top under the high-flux conditions. On the other hand, Issangya et al. (1999) reported higher values of 2–10 in the upper section of their high-density riser. This appears not to be consistent with our observations. When examining our and their results closely, however, one can find that the slip factors from the two studies are very similar at the same axial location under similar operating conditions because their riser is much shorter. Therefore, the values of the slip velocity and slip factor depend significantly on the respective height where the measurements were conducted. Issangya (1998) also reported higher values of a slip factor of 3–10 in the bottom section, consistent with our findings here.

Figure 6a also shows that the slip velocity increases with the gas velocity in the entire riser. In the bottom section of the riser, the slip velocity either does not change with G_s or only changes slightly with increasing G_s from 300 to 400 kg/m^2·s, but does not seem to change further from a G_s of 400 kg/m^2·s to 550 kg/m^2·s. The latter is consistent with the observations of Issangya et al. (1999), who reported the slip velocity reaching a plateau with increasing G_s. For the upper section (6 m and up) of our riser (beyond their riser of length 6.3 m l), however, our results (Figure 6a) show that increasing the solids circulation rate clearly led to an increase in the slip velocity. This is because increasing G_s increases the solids holdup, and therefore increases the tendency of solids aggregation. Larger and more frequent solids aggregation (clustering) decreases the effective drag between the gas and particles, resulting in higher slip.

To further illustrate the last point, the same data are plotted against the average solids holdup in Figure 6b, where the one-dimensional slip velocity is clearly shown to increase with the solids holdup. In addition, it is interesting to note the increase of the slip velocity with decreasing G_s under the same solids holdup. This is reasonable since the average solids velocity must be higher under higher G_s to achieve the same solids holdup, which in turn leads to lower slip velocity under the same U_g. Issangya et al. (1999) suggested that the solids circulation rate has no influence on slip velocity when the solids holdup is beyond 15%. While this is not entirely supported by our observations here, our results do show that the effect of G_s becomes smaller with the increase of solids holdup. Figure 6b also reports a significant increase of slip velocities with the increase of U_g, consistent with the observations of Issangya et al. (1999).

Axial variations of solids concentration in the high-flux riser

Figure 7 plots the axial profiles of the mean solids holdups for various high-flux ($G_s \geq 300$ kg/m^2·s) and low-flux ($G_s =$ 100 kg/m^2·s) operating conditions obtained in our study (solid symbols), by averaging the local solids holdups measured at 10 radial positions (excluding the center point) with the fiber-optic concentration probe at each axial elevation. Along the riser, these longitudinal files may be divided into four sections: the bottom dense section with solids holdups of about 20% or higher, a middle section with intermediate solids holdups of about 7–8% to 15–20%, a dilute section where the holdup is typically about 3–5%, and a top exit section where the holdup is somewhat higher than the dilute section due to the exit effect (which is minor due to the smooth exit). If we ignore the small top section due to possible exit effect and the small reduction of solids holdup at the 1.53-m level due to the entrance effect, there are three representative sections along the riser: the bottom dense section, the middle section of intermediate density, and the upper dilute section. For the low-flux operation ($G_s = 100$ kg/m^2·s), the middle section typically does not exist, so that the profile reduces to the typical S-shaped axial profile observed by many previous researchers (Li and Kwauk, 1980; Bai et al., 1992). The only other studies that also reported such a three-region longitudinal solids distribution are those of Issangya et al. (1997a,b, 1999), also obtained under high-density (and also high-flux) conditions. However, the existence of the top dilute section is not always clearly shown in their work because of the short riser.

Apparently, such a three-section profile, and the respective heights of these sections, are related to the high-flux opera-

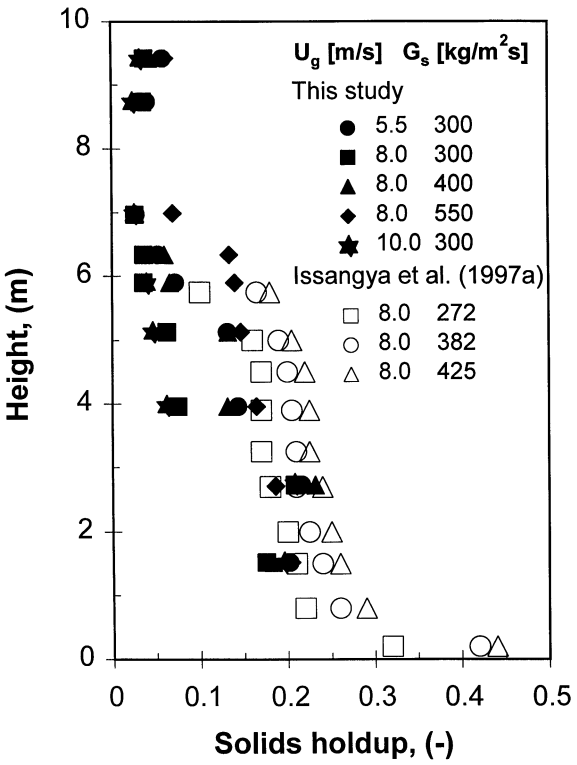

Figure 7. Axial solids holdup distributions in our 10.0-m high riser vs. 6.3-m high riser of Issangya et al. (1997a).

tion. This can be supported by the expansion of the middle section with the increase of the overall solids flux (G_s). For example, under $U_g = 8.0$ m/s, the middle section expands from minimal at $G_s = 300$ kg/m^2·s, to about 2 m long at $G_s = 400$ kg/m^2·s, and then to about 4 m long at $G_s = 550$ kg/m^2·s. Decreasing superficial gas velocity from 10.0 m/s and 8.0 m/s to 5.5 m/s has a similar effect. The length of this middle section may also be partly related to the total solids inventory due to the overall pressure balance in the loop of the riser and downcomer (Bi and Zhu, 1993), but firm conclusions can only be made when more data become available. For industrial designs, knowledge on the effect of solids flux (G_s) on the respective heights of these three axial sections in a long riser is very useful, since the solids flux varies widely (from 400 kg/m^2·s to 1,200 kg/m^2·s) in the industrial reactors.

Distinctions between low-flux and high-flux risers and between high-flux and high-density risers

As has been revealed from the discussion in the previous sections, there seem to exist certain similarities plus some dissimilarities between the flow characteristics of the high-flux circulating fluidized bed (HFCFB) in this study and those of the high-density circulating fluidized bed (HDCFB) reported by Issangya et al. (1997a,b, 1998, 1999, 2000), even though the operating conditions appear to be very similar. Therefore, it is necessary to examine the two situations more closely: besides the same riser and downcomer diameters and the similar G_s and U_g used in the two series of studies (the operating ranges of G_s and U_g in their studies were actually both somewhat lower, but there are enough overlap between the two), their riser is shorter (6.1 m vs. our 10 m) and their downcomer-to-riser height ratio much larger (1.4 vs. our 1.0). In addition, their total solids inventory is also twice as large (700 kg vs. our 350 kg), although their combined riser and downcomer volume is about 20% smaller. According to the theoretical analysis of Bi and Zhu (1993), both increased downcomer-to-riser height ratio and increased solids inventory in the system have the potential to increase the solids holdup in the riser and to increase the height of the denser sections (including the bottom dense section and the middle intermediate density section here). Combined with their shorter riser length, the differences just noted will effectively increase the overall solids holdup in their riser. This can be confirmed by comparing the longitudinal solids distribution profiles obtained in their studies with those of our studies (Figure 7). For example, comparing their profiles at $G_s = 382$ and 425 kg/m^2·s with our profile at $G_s = 400$ kg/m^2·s (both under $U_g = 8.0$ m/s), one can see that (1) their middle section is much longer ($\sim$4 m vs. $\sim$2 m), (2) their middle section is much denser ($\sim$20% vs. $\sim$12%), and (3) their middle section takes up much of the shorter riser. Because of the last point, most of the riser is in the middle section under $G_s = 382$ and 425 kg/m^2·s, so that the typical radial flow characteristics in their high-density riser resembles those observed only in the (much smaller) middle section in our riser.

Then, is high-flux operation really different from high-density operation? To answer this question, we should review both definitions first. The concept of high-density operation was first proposed by Bi and Zhu (1993) to distinguish the high-flux and high-density operating conditions encountered in most industrial risers (such as FCC risers) from those low-flux and low-density operations studied in most laboratory risers. Solids flux of over 200 kg/m^2·s was used to distinguish a high-flux operation. In their follow-up work, Zhu and Bi (1995) used $G_s > 200$ kg/m^2·s and $\epsilon_s > 3$–5% in the developed section of the riser to demarcate high-density operation from the low-density one. After a series of comprehensive studies on the high-density riser, Grace et al. (1999) further defined the high-density operation as "operations with $G_s >$ 200 kg/m^2·s and $\epsilon_s > 10\%$ throughout the entire riser." To characterize the flow behaviors inside the high-density riser, Grace et al. (1999) proposed a new dense suspension upflow (DSU) regime "where there is net upflow of solids across the entire riser, … and overall solids concentration of order 15 to 25% by volume, with little axial variation."

It is clear that what we have seen here in the high-flux riser does not match the DSU regime, even though the two key operating conditions, G_s and U_g, are the same. On the other hand, the flow structure in the middle intermediate density section observed in our study corresponds well with the DSU regime. For example, the net solids flux is clearly upwards at all radial positions, the same as in the DSU regime but different from the FF regime where there is downflow. The radial solids concentration profiles and slip factors are also very similar, though not entirely identical, to those in DSU.

It therefore appears that the DSU regime best describes the flow structure in the middle section of the high-flux riser, rather than the entire high-flux riser. This is seen more obviously seen in our longer riser than their shorter one. From Figure 7, however, one can already see the reduction of the solids holdup near the top of their shorter riser. For example, at $G_s = 272$ kg/m^2·s, the solids holdup begins to decrease quickly at $z = 5$ m, giving an obvious dilute section at the top. Therefore, it is reasonable to assume that such a dilute section also would appear for higher G_s if their riser had been longer.

Consequently, a high-flux operation may not necessarily lead to a high-density condition in a taller riser, since the upper dilute section will become longer in a taller riser and reduce the average solids holdup in the riser. Similarly, a high-density operation can be achieved more easily in a shorter riser. For example, if our riser were only 6 m long, the riser would be definitely operating under the high-density condition and within the DSU regime for $G_s = 400$ kg/m^2·s, as in their shorter riser. Therefore, whether a high-flux riser becomes a high-density riser (where the solids concentration is above 10% throughout the riser) is very much riser height dependent. Similarly, whether a high-flux riser operates mainly in the DSU regime is also dependent on the riser height, among others.

As shown in Figure 7, the cross-sectional mean solids concentration decreases to about 8% at a height of 7 m under the highest G_s of 550 kg/m^2·s. If the riser were only 7 m tall, the entire riser would be operating in the DSU regime. With this method, one can find the maximum height of the riser that would guarantee its operation in the DSU regime. The results are plotted in Figure 8 against the solids-to-air flow ratio for a fixed total solids inventory of 350 kg. It shows that the section for DSU operation increases with increasing solids-to-air flow ratio. In our 10-m riser, at least a solids-to-air ratio of over 80 would be required to fully establish the DSU regime with a solids inventory of 350 kg. This represents a G_s of 770 kg/m^2·s under $U_g = 8.0$ m/s. If more solids inventory is added into the downcomer, the axial solids distribution in the riser may be forced to adjust itself (to increase) to satisfy the new pressure balance (Bai et al., 1997), potentially leading to a longer section of DSU operation with a higher back pressure from the downcomer side.

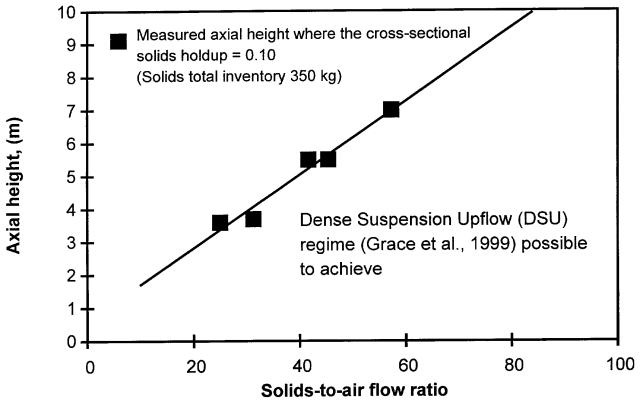

Figure 8. Conditions for a high-flux riser to operate as a high-density riser where the DSU regime would occupy the entire riser.

To summarize, the DSU describes the flow structure in the middle section of the high-flux riser with solids holdups between 10 and 25%, rather than the entire high-flux riser. A high-flux operation does not always lead to a high-density operation. With a shorter riser and/or higher solids inventory, the overall solids holdup under the same G_s and U_g would be higher, so that a high-flux riser would be more likely to operate under high-density conditions (with overall solids holdup higher than 10%). On the other hand, a high-density operation cannot be achieved without a high solids circulation rate (solids flux). In other words, high-flux operation or HFCFB is the necessary but not the sufficient condition for high-density operation or HDCFB. A high-flux operation that is also a high-density operation is more likely to fall in the DSU regime. What regime a high-flux operation that does not satisfy the high-density operation condition falls in is a good subject of further study. It is premature to define a new regime with the limited understanding we have so far, but it also may not be appropriate to still consider it in the FF regime.

Conclusion

A large set of measurements were performed in a high-flux (up to 550 kg/m^2·s) riser to study the solids holdup distribution and the flow development, using a fiber optic probe on eight axial levels in a 76-mm-ID and 10 m riser. The results show fewer uniform radial solids concentration profiles at high solids fluxes of over 300 kg/m^2·s than those obtained at lower fluxes of less than 200 kg/m^2·s. For both low- and high-flux operating conditions, the solids concentration remains low and relatively constant at the riser center throughout the riser, suggesting very quick solids flow development in the riser center at the bottom section. In the wall region, however, the flow development is significantly slower, with the solids holdup near the wall decreasing slowly toward the riser top. Increasing solids flux prolongs the solids flow development.

The one-dimensional slip velocity under high solids flux operations is shown to decrease from the bottom to the top of the riser and to increase with both solids flux and gas velocity. Correspondingly, the slip factor decreases from 6–10 at the bottom to 1.3–4 near the top of the riser.

To realize a high-density circulating fluidized-bed (HDCFB) operation, a high-flux circulating fluidized-bed (HFCFB) operation is essential but not sufficient. In the HFCFB, a new middle section with intermediate solids holdups of about 7% to 20% was found between the bottom dense section and the top dilute section normally observed in low-flux conditions. This section operates in a high-density condition and resembles the flow characteristics of the DSU proposed by Grace et al. (1999). The length of this middle section increases with the solids circulation rate, but decreases with the gas velocity. When its length extends to the riser top, however, a (HDCFB) forms.

Acknowledgment

Financial support from the Natural Sciences and Engineering Research Council of Canada is greatly acknowledged. One of the au-

thors (J.H.P.) also acknowledges the scholarship provided by Neste Research Foundation. The design of the pilot CFB system was assisted by J. Bu, and its construction was carried out by J. Wen and C. Cook. The help from A. Trikha, H. Zhang, J. Ball, A. Yan, S. Manyele, and S. Bodin during the experiments is also full greatfully acknowledged.

Notation

G_s = solids circulation rate, kg/m^2·s
r = radial distance from riser axis, m
R = radius of riser, m
U_g = superficial gas velocity, m/s
z = height from the riser bottom, m
ρ_p = particle density, kg/m^3

Literature Cited

Arena, U., A. Camomarota, L. Massimilla, and L. Pistane, "The Hydrodynamic Behaviour of Two Circulating Bed Units of Different Sizes," *Circulating Bed Technology II*, P. Basu and J. F. Large, eds., Pergamon Press, Oxford, p. 223 (1988).

Azzi, M., P. Turlier, J. F. Large, and J. R. Bernard, "Use of a Momentum Probe and Gammadensitometry to Study Local Properties of Fast Fluidized Beds," *Circulating Fluidized Bed Technology II*, P. Basu, M. Horio, and M. Hasatani, eds., Pergamon Press, Oxford, p. 189 (1991).

Avidan, A. A., "Fluid Catalytic Cracking," in *Circulating Fluidized Beds*, J. R. Grace, A. A. Avidan, and T. M. Knowlton, eds., Blackie, London, p. 466 (1997).

Bader, R., J. Findlay, and T. M. Knowlton, "Gas/Solids Flow Patterns in a 30.5-cm-Diameter Circulating Fluidized Bed," *Circulating Fluidized Bed Technology II,* P. Basu and J. F. Large, eds., Pergamon Press, Oxford, p. 123 (1988).

Bai, D.-R., Y. Jin, Z.-Q. Yu and J.-X. Zhu, "The Axial Distribution of the Cross-Sectionally Averaged Voidage in Fast Fluidized Beds," *Powder Technol.*, **71**, 51 (1992).

Bai, D., A. S. Issangya, J.-X. Zhu and J. R. Grace, "Analysis of the Overall Pressure Balance Around a High-Density Circulating Fluidized Bed," *Ind. Eng. Chem. Res.*, **36**, 3898 (1997).

Berruti, F., J. Chaouki, L. Godfroy, T. S. Pugsley and G. S. Patience, "Hydrodynamics of Circulating Fluidized Bed Risers: a Review," *Can. J. Chem. Eng.*, **73**, 579 (1995).

Bi, H.-T., J. Zhu, Y. Jin, and Z.-Q. Yu, "Forms of Particle Aggregations in CFB, Proc. Chinese National Conf. on Fluidization," Wuhan, China, p. 162 (1993).

Bi, H., and J.-X. Zhu, "Static Instability Analysis of Circulating Fluidized Beds and Concept of High-Density Risers," *AIChE J.*, **39**, 1272 (1993).

Contractor, R. M., G. S. Patience, D. I. Garnett, H. S. Horowitz, G. M. Sisler, and H. E. Bergna, "A New Process for n-Butane Oxidation to Maleic Anhydride Using a Circulating Fluidized-Bed Reactor," *Circulating Fluidized Bed Technology IV*, A. Avidan, ed., AIChE, New York, p. 387 (1994).

Derouin, C., D. Nevicato, M. Forissier, G. Wild, and J.-R. Bernard, "Hydrodynamics of Riser Units and Their Impact on FCC Operation," *Ind. Eng. Chem. Res.*, **36**, 4504 (1997).

Grace, J. R., A. S. Issangya, D. Bai, H-T. Bi, and J.-X. Zhu, "Situating the High-Density Circulating Fluidized Bed," *AIChE J.*, **45**, 2108 (1999).

Issangya, A. S., D. Bai, J. R. Grace, K. S. Lim, and J.-X. Zhu, "Flow Behavior in the Riser of a High-Density Circulating Fluidized Bed," *AIChE Symp. Ser.*, **93**(317), 25 (1997a).

Issangya, A. S., D. Bai, H. T. Bi, K. S. Lim, J. Zhu, and J. R. Grace, "Axial Solids Holdup Profiles in a High-Density Circulating Fluidized Bed Riser," *Circulating Fluidized Bed Technology V*, M. Kwauk and J. Li, eds., Science Press, Beijing, p. 60 (1997b).

Issangya, A. S., "Flow Dynamics in High Density Circulating Fluidized Beds," PhD Diss., Univ. of British Columbia, Vancouver B.C., Canada (1998).

Issangya, A. S., D. Bai, J. R. Grace, and J. Zhu, "Solids Flux Profiles in a High Density Circulating Fluidized Bed Riser," *Fluidization IX*, L. S. Fan and T. M. Knowlton, eds., Engineering Foundation, New York, p. 197 (1998).

Issangya, A. S., D. Bai, H. T. Bi, K. S. Lim, J. Zhu, and J. R. Grace, "Suspension Densities in a High-Density Circulating Fluidized Bed Riser," *Chem. Eng. Sci.*, **54**, 5451 (1999).

Issangya, A. S., J. R. Grace, D. Bai, and J. Zhu, "Further Measurements of Flow Dynamics in a High-Density Circulating Fluidized Bed Riser," *Powder Technol.*, **111**, 104 (2000).

Issangya, A. S., J. R. Grace, D. Bai, and J. Zhu, "A Local Voidage Correlation for CFB Risers," *Can. J. Chem. Eng.*, **79**, 279 (2001).

Karri, S. B. R., and T. M. Knowlton, "A Comparison of Annulus Solids Flow Direction and Radial Solids Mass Flux Profiles at Low and High Mass Fluxes in a Riser," in *Circulating Fluidized Bed Technology VI*, J. Werther, ed., Dechema, Frankfurt, p. 71 (1999).

Knowlton, T., "Interaction of Pressure and Diameter on CFB Pressure Drop and Holdup," *Workshop on Modeling and Control of Fluidized Bed Systems*, Hamburg (1995).

Li, Y., and M. Kwauk, "The Dynamics of Fast Fluidization." *Fluidization*, J. R. Grace and J. M. Matsen, eds., Plenum Press, New York, p 537 (1980).

Liu, J., J. R. Grace, H. Bi, H. Morikawa, and J. Zhu, "Gas Dispersion in Fast Fluidization and Dense Suspension Upflow," *Chem. Eng. Sci.*, **54**, 5441 (1999).

Martin, M. P., P. Turlier, and J. R. Bernard, "Gas and Solid Behaviour in Cracking Circulating Fluidized Beds," *Powder Technol.*, **70**, 249 (1992).

Matsen, J. M., "Some Characteristics of Large Solids Circulation Systems," *Fluidization Technology*, D. L. Keairns, ed., Hemisphere, New York, p. 135 (1976).

Ouyang, S., and O. E. Potter, "Consistency of Circulating Fluidized Bed Experimental Data," *Ind. Eng. Chem. Res.*, **32**, 1041 (1993).

Pärssinen, J. H., and J.-X. Zhu, "Particle Velocity and Flow Development in a Long and High-Flux Circulating Fluidized Bed Riser," *Chem. Eng. Sci.*, in press (2001).

Patience, G. S., J. Chaouki, F. Berruti, and R. Wong, "Scaling Considerations for Circulating Fluidized Bed Risers," *Powder Technol.*, **72**, 31 (1992).

Pugsley, T. S., F. Berruti, L. Godfroy, J. Chaouki, and G. S. Patience, "A Predictive Model for the Gas-Solid Flow Structure in Circulating Fluidized Bed Risers," *Circulating Fluidized Bed Technology IV*, A. A. Avidan, ed., AIChE, New York, p. 40 (1994).

Pugsley, T. S., B. J. Milne, and F. Berruti, "An Innovative Non-Mechanical Solids Feeder for High Solids Mass Fluxes in Circulating Fluidized Bed Risers," *Powder Technol.*, **88**, 123 (1996).

Schlichthaerle, P., and J. Werther, "Axial Pressure Profiles and Solids Concentration Distributions in the CFB Bottom Zone," *Chem. Eng. Sci.*, **54**, 5485 (1999).

Sapre, A. V., P. H. Schipper, and F. P. Petrocelli, "Design Methods for FCC Feed Atomization," AIChE Symp. Ser., **88**(291), 103 (1992).

Tanner, H., J. Li, and L. Reh, "Radial Profiles of Slip Velocity Between Gas and Solids in Circulating Fluidized Beds," *AIChE Symp. Ser.*, **90**(310), 105 (1994).

Van Landeghem, F., D. Nevicato, I. Pitault, M. Forissier, P. Turlier, C. Derouin, and J. R. Bernard, "Fluid Catalytic Cracking: Modelling of an Industrial Riser," *Appl. Catal. A: Gen.*, **138**, 381 (1996).

Van Swaaij, W. P. M., C. Buurman, and J. W. van Breugel, "Shear Stresses on the Wall of a Dense Phase Riser," *Chem. Eng. Sci.*, **25**, 1818 (1970).

Van Zoonen, D., "Measurement of Diffusional Phenomena and Velocity Profiles in a Vertical Riser," *Proc. Symp. on the Interaction Between Fluids and Particles," London*, p. 64 (1962).

Viitanen, P. I., "Tracer Studies on a Riser Reactor of a Fluidized Catalytic Cracking Plant," *Ind. Eng. Chem. Res.*, **32**, p. 577 (1993).

Wei, F., H. F. Lin, Y. Cheng, Z. W. Wang, and Y. Jin, "Profiles of Particle Velocity and Solids Fraction in a High-Density Riser," *Powder Technol.*, **100**, 183 (1998).

Yang, G., F. Wei, Y. Jin and Z. Yu, "Radial Solids Fraction Profiles in Inlet Region of High Density Circulating Fluidized Bed," *Chem. Eng. Technol.*, **20**, 304 (1997).

Zhang, H., P. M. Johnston, J.-X. Zhu, H. I. de Lasa, and M. A. Bergougnou, "A Novel Calibration Procedure for a Fibre Optic Concentration Probe," *Powder Technol.*, **100**, 260 (1998).

Zhu, J.-X. and H.-T. Bi, "Distinctions Between Low Density and High Density Circulating Fluidized Beds," *Can. J. Chem. Eng.*, 73, 644 (1995).

Zhu, J.-X., G-Z. Li, S-Z. Qin, F-Y. Li, H. Zhang, and Y.-L. Yang, "Direct Measurements of Particle Velocities in a Circulating Fluidized Bed Using a Novel Optical Fibre Probe," *Powder Technol.*, **115**, 184 (2001).

Manuscript received Nov. 22, 2000, and revision received Apr. 26, 2001.